Local and global expansivity in water

Jan Philipp Gabriel ✉ Ⓘ ; Robin Horstmann Ⓘ ; Martin Tress ✉ Ⓘ
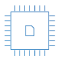
Check for updates

View Online   Export Citation

AIP Publishing

Local and global expansivity in water

View Online   Export Citation   CrossMark

Jan Philipp Gabriel,[1,a] (iD) Robin Horstmann,[2] (iD) and Martin Tress[3,a] (iD)

AFFILIATIONS

[1] Institute of Materials Physics in Space, German Aerospace Center, 51170 Köln, Germany
[2] Institute for Condensed Matter Physics, Technical University Darmstadt, 64289 Darmstadt, Germany
[3] Peter Debye Institute for Soft Matter Research, Leipzig University, 04103 Leipzig, Germany

Note: This paper is part of the JCP Special Topic on Water: Molecular Origins of its Anomalies.
[a] Authors to whom correspondence should be addressed: jan.gabriel@dlr.de and martin.tress@uni-leipzig.de

ABSTRACT

The supra-molecular structure of a liquid is strongly connected to its dynamics, which in turn control macroscopic properties such as viscosity. Consequently, detailed knowledge about how this structure changes with temperature is essential to understand the thermal evolution of the dynamics ranging from the liquid to the glass. Here, we combine infrared spectroscopy (IR) measurements of the hydrogen (H) bond stretching vibration of water with molecular dynamics simulations and employ a quantitative analysis to extract the inter-molecular H-bond length in a wide temperature range of the liquid. The extracted expansivity of this H-bond differs strongly from that of the average nearest neighbor distance of oxygen atoms obtained through a common conversion of mass density. However, both properties can be connected through a simple model based on a random loose packing of spheres with a variable coordination number, which demonstrates the relevance of supra-molecular arrangement. Furthermore, the exclusion of the expansivity of the inter-molecular H-bonds reveals that the most compact molecular arrangement is formed in the range of ~316 – 331 K (i.e., above the density maximum) close to the temperature of several pressure-related anomalies, which indicates a characteristic point in the supra-molecular arrangement. These results confirm our earlier approach to deduce inter-molecular H-bond lengths via IR in polyalcohols [Gabriel et al. J. Chem. Phys. 154, 024503 (2021)] quantitatively and open a new alley to investigate the role of inter-molecular expansion as a precursor of molecular fluctuations on a bond-specific level.

I. INTRODUCTION

The macroscopic properties of a liquid, such as its shear viscosity or its surface tension, are controlled by the dynamics, the interactions, and the arrangement of its molecules. However, the particular relations between the macroscopic and the molecular quantities are often obscured by the fact that the molecular properties are interconnected to each other through complicated and, in part, even unknown relations. In simple model liquids, the dynamics of the molecules have been connected to the mass density of the system.[1–3] However, many experimental studies of real materials show that such a relation is not unambiguously applicable; especially hydrogen (H) bonding systems cannot be described in this way.[4–7] This indicates that other factors beyond the average mass density, such as the particular supra-molecular structure, may also affect liquid dynamics on the molecular and, thus, in turn, on the macroscopic scale. Consequently, a comprehensive understanding of the dynamics and its thermal evolution in the liquid state and

also in the glass requires detailed insight into the supra-molecular structure and its changes with temperature.[8]

Among all materials, water is one of the most-studied liquids in any aspect, ranging from (but not limited to) structural investigations by means of x-ray[9–16] and neutron scattering,[14,16,17] examination of inter-molecular interactions using vibrational spectroscopy,[18–22] and also computer simulations testing different classical and quantum mechanical models.[20,23–27] Thereby, the coordinated inter-molecular H-bond is the central interaction, and its importance for the various anomalies of the material itself[28–30] as well as the sophisticated structure formation of biological molecules in an aqueous solution[16,31,32] has led to an exceptional research interest.

However, for most other liquids, no such vast collection of structural and dynamical data as well as theoretical model data exists. Therefore, we aim to develop a time- and cost-effective approach to obtain deeper insight into the supra-molecular structure of liquids. An earlier attempt has revealed intricate insights into

16 August 2024 13:35:19

the bond-specific expansivity of polyalcohols and, in turn, offered a clear explanation for the severed connection between their density and molecular relaxation dynamics.[33]

To explore the scope of this approach in depth, water represents a well-known reference system with many data collections in the literature for verification. Furthermore, water has a simple molecular structure, which rules out any conformational changes. Because of that, the supra-molecular aggregate is exclusively composed of a network of inter-molecular H-bonds, and the structural parameters are only its length and the orientation of the molecules with respect to each other (which results in the formation of a particular average number of inter-molecular H-bonds per molecule).

Here, we present an investigation of H-bond stretching vibrations of H_2O and HDO diluted in D_2O employing experiments and molecular dynamics simulations, which both aim at testing whether the correspondingly extracted bond lengths truly can describe macroscopic lengths and expansions. The obtained spectra exhibit pronounced contributions from combined vibrations, which are strongly suppressed in dilute HDO, where mostly the vibrations of isolated OH bonds prevail. Following the implication that only the latter reflects the actual state of the bond, we also draw more general conclusions on the interpretation of the vibrational spectra of H_2O in favor of contributions from isolated and combined vibrations instead of splitting into different states characterized by the number of donor and acceptor molecules in the direct vicinity. Furthermore, feeding an elementary model based on a random loose packing of spheres with the obtained bond lengths and the macroscopic mass density yields an average coordination number of 3.5–3.6, which is well in line with the literature. This confirms our assumption regarding the reliability of molecular length deduced from vibrational spectra and opens a new alley to investigate inter-molecular expansion as a precursor of molecular fluctuations on a bond-specific level.

II. MATERIALS AND METHODS

A. H_2O and HDO in D_2O

MilliQ water with a specific resistivity of 12 MΩ cm was used in the H_2O experiments. A solution of 2% HDO in D_2O was prepared by mixing 1 wt. % MilliQ water in D_2O (used as received from Sigma Aldrich). The mass densities of H_2O and D_2O were taken from Ref. 34 [using Eq. (1) of that reference] and Ref. 35, respectively.

B. Infrared spectroscopy measurements

IR spectra were recorded with a Fourier transform infrared (FTIR) spectrometer (Bio–Rad FTS 6000) combined with an IR microscope (UMA 500) and a liquid nitrogen-cooled mercury–cadmium–telluride (MCT) detector (Kolmar Technologies, Inc., USA), while a closed liquid cell with calcium fluoride windows (TC Demountable Liquid Transmission Cell, Harrick Scientific Products Inc.) was used to control the sample temperature.

C. Molecular dynamics simulations

The simulations of water employed the TIP4P/2005f water model,[36] an extension of the very successful TIP4P/2005 water model with a flexible geometry to address IR absorption. Thereby, the intra-molecular OH bond lengths are described by a Morse

potential, and a harmonic potential is used for the intra-molecular HOH angle. The parameterization of these potentials leads to good agreement with experimental results for the bending and stretching motions. These vibrations, together with the point charges on the hydrogen atoms and the additional site of the negative charge in relative positions to all three atoms, lead to oscillations of the molecular dipole moment in the IR range of the spectrum.

A bulk water system consisting of 2000 molecules was studied by molecular dynamics (MD) simulations using the GROMACS[37,38] simulation package (version 2019.4). The temperature was set using the Velocity-Rescaling thermostat,[39] with a time constant of 1.3 ps, and the density was equilibrated at each temperature at a pressure of 1 bar with the Parrinello–Rahman barostat,[40] with a time constant of 2.3 ps and a compressibility of 4.5×10^{-5} bar. Lennard-Jones and Coulomb interactions were calculated up to a distance of 1.2 nm, and long-range interactions for both were calculated using the Particle-Mesh-Ewald method[41] and a Fourier-spacing of 0.144 nm. The integration step was $\Delta t = 0.2$ fs.

Equilibration simulation runs lasted at least 12 ns, extending up to 200 ns at lower temperatures to ensure a minimum mean-square displacement of 50 nm^2 across all temperatures. These were followed by 3.5 ns sampling simulations at constant mean densities for each temperature or until achieving a 20 nm^2 displacement, from which ten time-equidistant configurations with instantaneous velocities were selected as initial setups for 0.5 ns production runs, recorded every 2 fs. This approach allowed sampling from distinct micro-states and enabled the capture of higher frequency dynamics, averaging the outcomes across all production runs per temperature for the following analysis.

For the calculation of the IR spectra from these simulations, the classical representation with the Fourier transform of the autocorrelation of the total dipole moment was employed,[42]

$$I(\omega) \sim \int_{-\infty}^{\infty} dt e^{-i\omega t} \langle \vec{M}(0) \cdot \vec{M}(t) \rangle, \qquad (1)$$

where $\vec{M} = \sum_i \vec{\mu}_i$ is the total dipole moment of the system, and the angular brackets $\langle \cdot \rangle$ denote an ensemble average and averages over several time origins. The self-correlation spectra are obtained by taking only the summation $\sum_{i,j=i} \vec{\mu}(0) \cdot \vec{\mu}(t)$, i.e.,

$$I_{\text{self}}(\omega) \sim \int_{-\infty}^{\infty} dt e^{-i\omega t} \langle \vec{\mu}_i(0) \cdot \vec{\mu}_i(t) \rangle. \qquad (2)$$

The spectra were divided by temperature to compensate for its effect on the intensity of the absorption.

III. RESULTS

A. Experimental FTIR spectra of H_2O

The IR absorption spectra of H_2O contain a broad structured peak in the range between 3000 and 3700 cm^{-1}, which is generally assigned to stretching vibrations of OH groups, with the portion below ~3600 cm^{-1} reflecting those involved in inter-molecular H-bonds[43] [Fig. 1(a)]. As temperature decreases, the overall absorbance of this peak increases, and its maximum position at ~3400 cm^{-1} as well as its shoulders at ~3300 cm^{-1} and slightly below 3600 cm^{-1} shift to lower wavenumbers. This indicates a weakening of the covalent OH bond, which is typical for inter-molecular
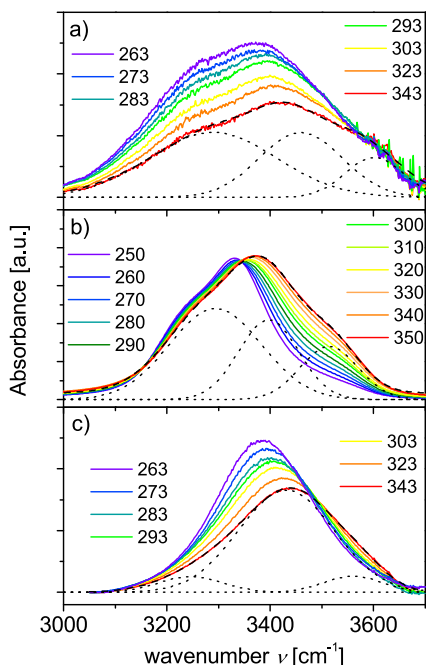
FIG. 1. Vibrational spectra in the OH-stretching range: (a) experimental IR absorption spectra of pure H_2O, (b) dipole self-correlation spectra of pure H_2O obtained from molecular dynamics simulation, and (c) 2% HDO in D_2O vibrations at different temperatures as indicated (in Kelvins). The dashed lines are exemplary fits to the spectra at the highest temperature in each panel composed of three Gaussians; these individual Gaussian contributions are shown separately as dotted lines.

H-bond forming materials since the increase in density brings the H-bond acceptor closer to the OH, thus stretching the interatomic potential of the covalent OH-bond.

According to the literature, the assignment of the various contributions of the structured OH stretching band is ambiguous and has been controversially debated.[43,44] Thereby, two opposing ideas appear to dominate: in one view, individual peaks of the complex band are considered to reflect states of a specific number of active donor and acceptor sites in the probed molecule[44] or to symmetric and antisymmetric stretching modes,[21] thus expecting a superposition of several Gaussian peaks reflecting the number of states;[45–49] the other interpretation distinguishes contributions originating either from isolated or collective vibrations; the latter ones are sometimes regarded as cross-correlations, combination bands, or coupled vibrations, in which case neither the precise number nor the exact shape is obvious.[24–26,43,50] The latter view has also been established in the terahertz range of H_2O absorption.[51] Essential for the present investigation is to unravel the contributions and identify which ones originate from isolated vibrations and, thus, can be reasonably related to the physical properties of individual bonds, e.g., their length.

B. Dipole correlation spectra of H_2O from MD simulations

Since the absorption of IR radiation is based on the presence of a transition dipole moment of matching transition energy,

the dipole correlation spectra of water were deduced from MD simulations [Fig. 1(b)]. Thereby, the self-correlation spectra of the molecules exhibit a remarkable resemblance with the experimental results, also consisting of three major contributions: a prominent peak in the center at about ~3400 cm^{-1}, which shifts significantly to lower wavenumbers as temperature decreases; a pronounced low-frequency-shoulder at ~3300 cm^{-1}; and a weaker shoulder at about ~3550 cm^{-1}, which increases in intensity as temperature rises. Although the experimental FTIR spectra are considerably broader, a feature that is often observed in simulations,[52] the peak positions of the three major contributions are quite similar.

Despite the fact that only the self-correlations were calculated, these simulated spectra are an intricate mixture of isolated and combined vibrations because a highly coupled system is modeled. The similarity to the experimental FTIR spectra suggests that the latter also contain a considerable contribution of collective vibrations (intra- and inter-molecular), which is not easily disentangled.

C. Experimental FTIR spectra of dilute HDO in D_2O

An experimental way to largely isolate the OH bond vibration, i.e., to minimize combination bands of collective vibrations, is to dissolve HDO in D_2O.[23,53] We examine a volume concentration of 2% HDO in D_2O, which means that statistically, there is one OH bond per 50 water molecules. Assuming an even distribution, this separates OH bonds by ~1.3 nm, which should strongly reduce energy transfer between these oscillators. The respective IR spectra exhibit a much narrower peak at ~3400 cm^{-1} than in the case of H_2O (although it is still broad compared to other absorption bands) with very little structure; only a slight asymmetry indicates the presence of additional contributions at lower and higher frequencies [Fig. 1(c)]. This confirms that the spectrum of H_2O indeed contains several contributions of combined vibrations and a single isolated vibrational peak.

Further evidence for this interpretation is provided by the rather unstructured peak shape one can observe in materials with lower concentrations of OH bonds, e.g., polyalcohols:[33] despite the fact that the formation of up to three inter-molecular H-bonds per oxygen (O) is possible (i.e., different states of coordination are possible), no additional shoulders are found. The spatial separation of the OH groups due to their attachment to a carbon backbone in these materials strongly reduces the correlation among the vibrations of the OH bonds.

D. Quantitative analysis of vibrational spectra

Despite past approaches to fit the OH-stretching region of H_2O with five or more Gaussians accounting for the potential number of donors and acceptors or other assumed molecular states,[45–49] a sum of three Gaussian functions appears to be sufficiently accurate to fit the measured and simulated spectra of H_2O and HDO in D_2O to extract peak position, width, and area of the individual contributions (Fig. 1). However, the close superposition of the contributions leads to a strong dependence on these fit parameters and, thus, large uncertainties. Consequently, we also fitted a polynomial curve to the spectra of HDO in D_2O to deduce the position of the maximum with much better precision (which, due to the suppressed contributions of collective vibrations, in this case, corresponds to the peak of the vibration of the individual bond).

To also improve the extraction of the width and area of the peaks in the spectra of HDO in D_2O, the fit with three Gaussian functions was repeated with the maximum position of the central peak fixed to the value obtained from the polynomial fits. Finally, the experimental H_2O spectra were fitted again with three Gaussian functions, with the width of the central peak fixed to the value obtained from the improved fit of the spectra of HDO in D_2O.

To deduce inter-molecular bond lengths, the peak position of the isolated vibration, i.e., the maximum at ~3400 cm^{-1}, of both systems is converted to the corresponding OH$\cdots$O length $D_{OH\cdots O}$ via an empirical relation that describes the correlation observed in a large data set of several H-bonding crystalline materials,[54,55]

$$D_{OH\cdots O}^{FTIR}(\bar{\nu}) = 13.21 \log\left(\frac{304 \cdot 10^9}{3592 - \bar{\nu} \cdot cm}\right) pm, \quad (3)$$

where $\bar{\nu}$ is the peak position in cm^{-1}, and the result is obtained in picometers (pm). Originally, this relation was established for crystalline solids; in liquids, on the other hand, the disordered structure only allows the determination of a statistical nearest neighbor distance from the radial pair correlation function without any information about the bond character along this distance. Nevertheless, due to the local nature of isolated vibrations in the inter-atomic potential, the relation given by Eq. (3) is expected to be independent of (long-range) structural order. Thus, it is considered to also hold liquids.[56,57] A similar approach has been taken in the past based on Raman spectra.[58,59] The extracted length is in the range of 280 pm, which is typical for the OH$\cdots$O distance in inter-molecular H-bonds. Furthermore, as expected for inter-molecular bonds, the length expands with increasing temperature for both pure H_2O and dilute HDO in D_2O.

In particular, the latter matches well with the average OH$\cdots$O distance along the inter-molecular H-bonds deduced from the coordinates of the molecules in the simulation. In contrast, an attempt to convert the frequency positions of the central peak of the simulated dipole correlation spectra through Eq. (3) yields a length that is about 5 pm smaller and, more importantly, much less steep. The latter demonstrates the limitations of the simulation in capturing details such as the correct temperature dependence of the relation between inter-molecular distance and respective vibrational absorption.

E. Crosscheck with mass density

In the past, several studies established a conversion from mass density ρ to the inter-molecular distance (even more specifically, the separate lengths of covalent and inter-molecular H-bonds were presented).[22,64,65] This is certainly motivated by the simple internal structure of the water molecule, which appears promising (if not mandatory) for linking the inter-molecular length scale with a macroscopic quantity, as attempted in the present study. Thereby, the inter-molecular H-bond length was considered to correspond to the average distance of nearest-neighbor pairs of oxygen atoms $D_{O\text{-}O}$, which for H_2O was estimated as[22,64,65]

$$D_{O-O}^{\rho}(H_2O) = 2.695 \times 10^{-7} g^{1/3} \rho^{-1/3}, \quad (4)$$

where the prefactor carries the cube root of grams $g^{1/3}$ as a unit. This equation should also be applicable to D_2O since it is governed

by similar inter-molecular interactions. To account for the difference in molecular mass, a correction factor of $\left(\frac{M_{D_2O}}{M_{H_2O}}\right)^{1/3}$ must be introduced,

$$D_{O-O}^{\rho}(D_2O) = 2.791 \times 10^{-7} g^{1/3} \rho^{-1/3}. \quad (5)$$

However, the thus obtained lengths using the temperature dependent mass densities of H_2O and D_2O[34,35] are in the range of ~270 pm for both, i.e., about ~10 pm shorter than we estimate for the length of the inter-molecular H-bonds from the FTIR data [Fig. 2(a)]. Furthermore, the temperature dependence is quite different, being non-monotonous with minima at 277 and 284 K, respectively, which indicates the density maxima of both materials,[66] in contrast to the monotonous increase in $D_{OH\cdots O}$ deduced from FTIR. Consequently, the direct conversion of mass density into inter-molecular H-bond length (or intra-molecular ones, for that matter)[22,64,65] is incorrect.
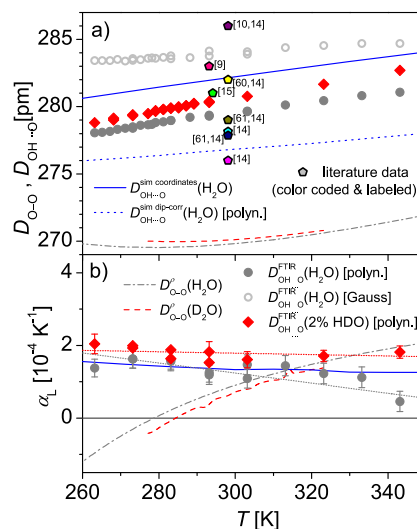
FIG. 2. (a) Inter-molecular H-bond length as function of temperature obtained from different approaches: calculated via Eq. (3) from the frequency of either the main Gaussian peak (open gray circles) or the global maximum deduced with a polynomial fit (solid gray circles) of the FTIR spectra of H_2O and 2% HDO in D_2O (solid red diamonds); and as coordinates from the MD simulations of H_2O (solid blue line). The dotted line corresponds to the converted maxima of dipole correlation peaks from the simulation deduced via a polynomial fit and Eq. (3). The dashed-dotted and dashed lines are average oxygen–oxygen (O–O) distances for H_2O and D_2O, respectively, calculated from the mass density[34,35] via Eqs. (4) and (5). In addition, several literature values of the first peak in the radial O–O pair correlation function deduced either from x-ray scattering[9,15] or from a combined analysis[14] of several older x-ray[10,60,61] and neutron scattering[62,63] data sets are shown. (b) Deduced linear expansion coefficient α_L of select data shown in (a) using the same symbols and color code; dotted red and gray lines are linear fits to the converted IR data of HDO in D_2O and H_2O, respectively. In order to reduce the scattering in the numerical differentiation, only data points in 10 K steps were included in (b). The experimental uncertainty in panel (a) is smaller than the symbol size; in panel (b), the uncertainty is displayed only for some representative data points for clarity.

IV. DISCUSSION

A. Sphere model

As is well-known, the unusual thermal evolution of the mass density of water is governed not simply by inter-molecular bond expansion but also by a complex structural reorganization.[67] To take this into account, we set up a slightly more complex yet still simplistic geometric model that approximates the water molecules as spheres, an approach that is supported by x-ray scattering results.[10] Thereby, the oxygen atom is in the center of the sphere with a radius equal to half the length of an inter-molecular H-bond (i.e., $r_s = 0.5 \times D_{\mathrm{OH} \cdots \mathrm{O}}$), and the hydrogen atoms are located roughly at the surface of this sphere corresponding to two of the edges of an inscribed tetrahedron (actually, the surface of the sphere, would cut the inter-molecular H-bond in half, which means that the covalently bound hydrogen atoms are considerably closer to the center).

In this picture, liquid water resembles a loose packing of these spheres with a coordination number of $Z \leq 4$; thereby, lower coordination numbers account for the time average of broken intermolecular H-bonds during the rearrangement of the network. (We would like to note that a random close packing of spheres corresponds to ~6 nearest neighbors, i.e., neighbors with direct contact; hence, an equivalent of a random loose packing has to be employed in our model. In simulations, random loose packing is achieved by considering spheres with surface friction[68]—not unlike the concept of molecular friction in liquids and glasses.) In a random loose packing, the number of nearest neighbors Z, i.e., the coordination number, is related to the volumetric space filling f_s of the spheres.[68] With the latter, we can relate the volume occupied by the spheres V_s to the total volume V_t as $V_s = f_s V_t$. Then, V_s can be replaced by the volume of a single sphere and V_t by the specific volume given by mass density ρ and molecular mass M_W, which yields

$$\frac{4}{3}\pi r_s^3 = f_s \frac{M_W}{\rho N_A}. \tag{6}$$

Consequently, the space-filling of the equivalent spheres can be estimated from the average distance between oxygen atoms of adjacent water molecules, $D_{\mathrm{OH} \cdots \mathrm{O}} = 2r_s$, as

$$f_s = \frac{\pi \rho N_A}{6 M_W} D_{\mathrm{OH} \cdots \mathrm{O}}{}^3. \tag{7}$$

With an empirical relation $Z(f_s) = 2 + 11 f_s^2$ taken from the literature,[69] the respective average sphere–sphere coordination numbers are obtained according to

$$Z = 2 + 11 \left(\frac{\pi \rho N_A}{6 M_W} \right)^2 D_{\mathrm{OH} \cdots \mathrm{O}}{}^6. \tag{8}$$

The resulting values are in the range of 3.5–3.6 for both H_2O and dilute HDO in D_2O. Although the respective values in the literature range from ~2 − 4,[11,30] the standard view seems to consider 3.5–3.6 H-bonds per molecule in liquid water.[27] For example, some x-ray diffraction data shows 4.4 neighbors in the first shell, although a considerable proportion of these are more than 3.3 Å apart, which means these are outside the typically considered cut-off length of inter-molecular H-bonds.[9] Using the cut-off criterion yields ~3.5 neighbors in the 2.8–3.3 Å range.[9,27] Hence, the values obtained via our simplistic model are reasonable and, thus, validate the employed approach to quantitatively extract inter-molecular distances from the FTIR band.

It is important to note that the equivalent sphere model intrinsically implies straight inter-molecular H-bonds, while in reality, these can be established over quite a range of angles.[55,65] Assuming that the frequency position of the OH stretching vibration is only sensitive to the proximity of an H-bond acceptor but not to the angle, the extracted $D_{\mathrm{OH} \cdots \mathrm{O}}$ may be overestimating the true distance depending on the angle. Inter-molecular H-bonds are established under angular deviations of up to 20° from the straight arrangement of oxygen–hydrogen–oxygen atoms.[70] In this extreme case, the true value is reduced by a factor of ~0.986, i.e., 1.4% shorter [pure geometric estimation using the length ratio φ between the covalent and the inter-molecular parts of the OH···O-bond and the angular deviation θ yields the equation for this correction factor $R = \frac{\varphi \cos(\alpha) + \cos(\theta - \alpha)}{\varphi + 1}$ with $\alpha = \arctan\left(\frac{\sin \theta}{\varphi + 1 - 2\sin^2(\theta/2)} \right)$]. Inserting this in Eq. (8) yields a systematic overestimation of Z of less than 4% for H-bonds with an angle of 160°.

Furthermore, the equivalent sphere model also does not take into account the tetrahedral arrangement of H-bonds around one oxygen atom. Instead, in the model, any sufficiently close adjacent sphere contributes to Z even if, in reality, no inter-molecular H-bond can be established (e.g., if the central oxygen atom has already formed four H-bonds or if no tetrahedral arrangement with the other H-bonds is achieved). Consequently, this will also lead to an artificial increase in the estimated coordination number.

Finally, the breakdown of the H-bond network in liquid water, which is indicated by the fact that the density of liquid water in a certain temperature range is higher than that of ice, suggests that the oxygen atoms of neighboring molecules might come closer than the H-bond distance. Such a configuration cannot be described with impenetrable spheres. Since this collapse of the H-bond network strongly varies with temperature dependence, we cannot expect the model to yield reliable insight into the temperature dependence of the coordination number. Considering these intrinsic inaccuracies of this rather simple model, the close match with the literature appears remarkable.

B. Thermal expansion

Although the sphere model reasonably links the intermolecular H-bond length with the macroscopic mass density, the temperature dependencies of the respective lengths exhibit a qualitative difference [Fig. 2(a)]. This has also been found in an earlier simulation study employing the TPI4P/2005 water model[71] (although its particular results exhibit considerable differences, as will be discussed later), and it emphasizes a fundamental difference between these two quantities. To examine this in more detail, we calculate the linear expansion coefficient α_L^{Hb} via the numeric derivative of the H-bond length,

$$\alpha_L^{Hb}(T) = \left(D_{\mathrm{OH} \cdots \mathrm{O}}^{FTIR}(T) \right)^{-1} \frac{\mathrm{d}}{\mathrm{d}T} D_{\mathrm{OH} \cdots \mathrm{O}}^{FTIR}(T). \tag{9}$$

Corresponding to the length derived from mass density, $D_{\mathrm{O-O}}^{\rho}$, the volumetric expansion coefficient α_V is calculated as

$$\alpha_V(T) = \rho(T) \frac{\mathrm{d}}{\mathrm{d}T} \rho(T)^{-1}, \tag{10}$$

16 August 2024 13:35:19

and the relation $\alpha_V = 3\alpha_L^g$ is used to obtain the linear expansion coefficient [Fig. 2(b)]. The inter-molecular H-bond length shows a weakly decreasing expansion coefficient of about $1.7–1.9 \times 10^{-4}$ K^{-1} in the measurements on dilute HDO and $1.3–1.5 \times 10^{-4}$ K^{-1} in the simulations of H_2O. In slight contrast, the experimental data of H_2O exhibit a considerable reduction from 1.8×10^{-4} to 0.5×10^{-4} K^{-1}, which may suggest that the contribution of collective bands in the respective FTIR spectra is too intense to reasonably extract minute characteristics of the isolated vibration.

A remarkable comparison is possible through studies of amorphous water at low temperatures; both molecular dynamics simulations (using a TIP5P-E water model)[72] and small angle neutron scattering measurements of D_2O confined to nanopores of 15 Å diameter[73] show a density minimum at a temperature of about 250 K below which a positive expansivity is observed. Since no rearrangements in the supra-molecular structure are expected in this range, one might hypothesize that the remaining expansivity should correspond to that of the inter-molecular H-bond. Indeed, the density data provided by the simulations and the measurements of confined water yield linear expansion coefficients of 1.2×10^{-4} and 0.5×10^{-4} K^{-1}, respectively, well in line with the values we find.

In contrast to the purely positive values of the thermal expansion coefficient we find for the inter-molecular H-bond length in the range $0.5–1.9 \times 10^{-4}$ K^{-1} at the studied temperatures, those obtained from the mass density show values varying from -1.5×10^{-4} K^{-1} at 260 K to 2×10^{-4} K^{-1} at 350 K.

In order to understand this, one has to also consider the supra-molecular arrangement and its changes in liquid water. It is well-known that the thermal expansion of water is dominated by orientational effects that enable certain packing structures rather than solely the thermally controlled position in the potential of inter-molecular interactions. However, a close inspection of the inter-molecular H-bond length reveals that the latter effect also contributes significantly to the macroscopic expansion [Fig. 2(b)]. In the context of supra-molecular arrangement, the expansion of the inter-molecular bond length can be viewed as the effective thermal expansion of the molecule (used here in the sense of the constitutional particles of the liquid). Consequently, one would expect the intersection point of the macroscopic expansion coefficient and one of the inter-molecular H-bonds ($\sim$331 K using the $D_{OH\cdots O}$ deduced from dilute HDO or $\sim$316 K from the simulated $D_{OH\cdots O}$) to indicate the temperature of the most compact structural order if the inter-molecular bond length was temperature independent (Fig. 3).

Because the water molecule has no internal rotational degrees of freedom and the supra-molecular structure is practically just an H-bond network, the global thermal expansion can easily be dissected into the contributions of structural reorganization and H-bond expansion. After an incremental temperature increase dT, the length of an aggregation of water molecules $L(T)$ expands to

$$L(T + dT) = \left(1 + dT\alpha_L^g(T)\right)L(T). \tag{11}$$

Note that Eq. (11) does not only hold for the global expansion but also the individual effects of structural and H-bond expansion when $\alpha_L^g(T)$ is replaced by the corresponding expansion coefficient of either contribution, i.e., $\alpha_L^{st}(T)$ and $\alpha_L^{Hb}(T)$, respectively. Since both contributions expand the system via an extension of the H-bond (either directly by stretching or indirectly by reorientation and
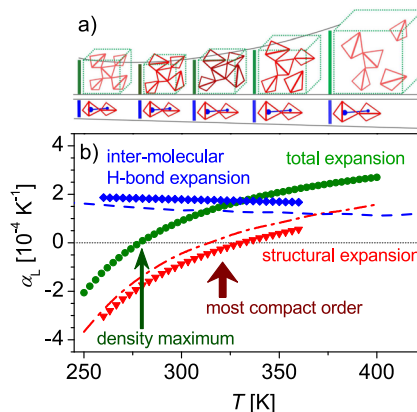
FIG. 3. (a) Schematic depiction of the parallel evolution of steadily increasing inter-molecular distance (visualized as the size of the red tetrahedrons and as a blue bar representing the effective extension of the water molecules and a single inter-molecular H-bond) and the non-monotonous structural expansion of the supra-molecular arrangement, which contributes to the total specific volume (green boxes and bars) of water. (b) Corresponding total linear thermal expansion coefficient α_L of water calculated from mass density[34] via Eq. (10) (green circles) and its separated components, i.e., the thermal expansion of the inter-molecular H-bonds deduced from IR measurements (blue diamonds) and MD simulations (blue dashed line), as well as the expansion due to structural reorganization, i.e., the difference between the expansion coefficients of the whole system and the H-bonds (red triangles and dashed-dotted line for experimental and simulation data, respectively). The vertical arrows indicate the approximate temperatures of the highest density and the most compact supra-molecular order.

straightening), the combined effect is then expressed by multiplying both pre-factors,

$$L(T + dT) = \left(1 + dT\alpha_L^{st}(T)\right)\left(1 + dT\alpha_L^{Hb}(T)\right)L(T). \tag{12}$$

Comparing Eqs. (11) and (12) yields

$$\alpha_L^g = \alpha_L^{st} + \alpha_L^{Hb} + dT\alpha_L^{st}\alpha_L^{Hb} \approx \alpha_L^{st} + \alpha_L^{Hb}, \tag{13}$$

where the last approximation is based on $\alpha_L^{st}, \alpha_L^{Hb} \ll 1$. This justifies a simple additive approach to the identified contributions to thermal expansion in water.

In other words, subtracting the expansion coefficient of the inter-molecular H-bonds from the global one yields the expansivity of the supra-molecular structure, which is defined by the bond angles and the number of bonds per molecule but not by the inter-molecular bond length; previously, this has also been referred to as an anomalous contribution to the thermal expansion.[74] This leads to the picture that at low temperatures, the supra-molecular arrangement of liquid water contains a lot of "free" space—the well-known almost tetrahedral order of super-cooled water.[75] A temperature increase breaks the bonds, which gradually collapses the tetrahedral network and, thus, creates a more compact structure. Below a temperature of 277 K, this collapse exhibits a stronger temperature dependence than the length of the inter-molecular H-bonds (of course, this does not include the effects below 250 K, where again a positive expansion can be observed, e.g., in confined water[73]),

which causes the anomalous expansivity of liquid water. At 277 K, the expansion coefficients of the network collapse and the H-bond length cancel out, and a maximum in density is achieved. Upon further increase in the temperature up to ~320 K, the supra-molecular structure still collapses further but is outweighed by the expansion of the inter-molecular H-bonds, resulting in the normal behavior of the global expansivity (Fig. 3). Yet, only at ~320 K, the network has collapsed completely and a most compact arrangement has been achieved. At even higher temperatures, the changes in the supra-molecular network exhibit a positive expansivity, probably due to a reduction in the average number of inter-molecular H-bonds per molecule. Evidently, a highly characteristic supra-molecular structure is established in water at a temperature of ~320 K (and ambient pressure).

In fact, at about this temperature, several pressure-related anomalies can be observed in water: the compressibility exhibits a minimum (~320 K),[76] and the thermal expansivity is invariant of pressure (~316 K)[67,77,78] as is the difference between the heat capacities at constant pressure and constant volume $C_p - C_v$ (~313 ± 4 K),[67] the isothermal piezo-optic coefficient (the derivative of the refractive index with respect to pressure) has a minimum (~318 K),[79] the heat capacity at constant pressure C_p shows the smallest variation with pressure (~325 ± 10 K),[77] and the pressure dependence of the zero shear viscosity changes from monotonous increase to a curve with a minimum (~307 K).[80] It has been proposed earlier that the minimized susceptibility to pressure change revealed in these anomalies indicates the establishment of the most compact supra-molecular arrangement rather at the temperature of $T^* \approx 315$ K than at the actual density maximum.[67,77,78,81] As simulation studies suggested before,[82] our findings now confirm experimentally that, despite the different temperatures at which they occur, the density maximum and the mentioned pressure-related anomalies are caused by the same anomaly in the supra-molecular arrangement.

Despite the fact that these structural changes represent an additional component of global thermal expansion, water still has a relatively small expansion coefficient compared to most other molecular liquids.[8] This is because the contribution of the strong inter-molecular H-bonds is much smaller than the expansion of weaker bonds, such as van der Waals interactions or weak H-bonds, which typically dominate the expansivity of liquids, as has been shown for glycerol.[33]

We would like to note that a simulation study has already investigated the thermal evolution of the supra-molecular structure by separating the expansion of the inter-molecular H-bonds.[71] However, that work found a considerably larger expansion coefficient of the inter-molecular H-bond of about 4×10^{-4} K^{-1}. Not only is this value by a factor of 2 larger than the one we find here experimentally, but it also exceeds the global expansivity obtained from the mass density. Consequently, that work[71] reports a monotonously decreasing expansivity of the supra-molecular structural arrangement in the whole studied temperature range spanning 200–360 K. Since this range includes the temperature of the above-discussed pressure anomalies (~320 K), that study does not find the link between these anomalies and the density maximum. Thus, the results we report here are more plausible because they unravel this connection and specifically explain the lower temperature of the density anomaly.

C. Isotope effect

A remarkable aspect thereby is the gradual increase of the temperature at which the density maximum occurs as the atomic mass of the involved hydrogen isotope increases; for D_2O it is at ~284 K,[66] and for T_2O even ~287 K.[83] Considering that a higher mass of the hydrogen isotope results in a stronger covalent bond with the oxygen atom, a reduced thermal expansivity can be expected. With the simplistic assumption of the same contribution of the structural rearrangement to thermal expansivity, one can indeed explain an increased temperature of the cross-over point from negative to positive thermal expansivity.

However, experimental studies show that in D_2O, the inter-molecular H-bonds are stronger than in H_2O.[84] This also suggests a higher stability of the supra-molecular structure, which, on the one hand, would give rise to an additional increase in the cross-over temperature. On the other hand, stronger inter-molecular bonds are less susceptible to temperature, which would lead to a shallower slope of thermal expansivity. Then, the sum of the expansivity of the bond would shift stronger to lower temperatures, countering the other effects. Consequently, a qualitative assessment is insufficient to draw a final conclusion. Instead, quantitative investigations on D_2O similar to the one presented here for H_2O (including a correlation of the DO stretching vibration frequencies with the respective inter-molecular bond length) are required to resolve this question.

D. Relation to x-ray and neutron scattering data

The determination of the inter-molecular H-bond length in water has been the subject of several studies that employed x-ray or neutron scattering,[9–13,17] particularly the determination of the radial distribution function of oxygen atoms. The reported values for the average length of the nearest neighbor O–O distance are well within the range of our data, although the literature results exhibit quite some scattering [Fig. 2(a)]. While the data reported by Bergmann *et al.*[15] and Soper[14] are a near perfect match with our results, others are larger or smaller by up to 5 pm. However, it should be noted that due to negligence of the angular asymmetry of the H-bond, our results may systematically overestimate the length by up to 1.4%, or ~4 pm, i.e., putting them potentially in agreement with some of the lower literature values. Although all of these differences correspond to less than ±2% around the 281 pm-mark, this deviation is bigger than the thermal expansion we find for the inter-molecular H-bond in the temperature interval 260–350 K (expansion by ~3 pm or ~1%).

We would like to emphasize that water is a special case where, due to the simple structure of the individual molecule, the inter-molecular H-bond length can be easily evaluated from scattering methods probing the oxygen pair correlation function. However, for more complex molecules that engage in H-bonding, this is far more demanding—especially if intra-molecular conformational changes are possible. Particularly for these latter cases, the here presented analysis of vibrational spectroscopy data is a valuable addition to determining specifically the inter-molecular H-bond length. As has been demonstrated, the separate estimation of this quantity combined with information from the macroscopically deduced specific volume enables a better understanding of molecular packing and structural changes.

E. Implications for the IR spectra of water

Some of the relations and findings discussed above have notable consequences for the expected shape of the IR absorption band of the OH stretching vibration. Based on the correlation between the inter-molecular H-bond length and the peak position of the OH stretching band, one can conclude that the spectral shape of this band reflects the distribution of bond lengths in the system. Thereby, two opposing effects complicate the conversion. First, the nearest neighbor oxygen pair correlation function exhibits an asymmetry along the radial coordinate in the probability distribution of the first coordination shell.[12] In particular, the distribution is stretched toward longer distances, as demonstrated by the fact that the mean distance of the nearest neighbor is larger than the most probable distance. This would result in a skewed IR absorption band with an extended high-frequency flank. However, the conversion, according to Eq. (3), introduces another distortion due to its nonlinear shape. In this case, larger H-bond lengths are mapped onto a narrower frequency interval than short ones, which would result in a stretched low-frequency flank with reduced intensities, while the high-frequency flank would exhibit a compression in frequency but an increase in intensity. Although these two contributions have opposite effects, it is unlikely that they will cancel out. Consequently, a general expectation for the broad absorption band of the OH stretching vibration is, even without considering the sidebands from collective vibrations, an asymmetric shape. As a result, a fit to one or more Gaussian functions is unjustified not only from a physical point of view but may also deliver incorrect values of the peak position, as was demonstrated in the present investigation for the H_2O spectra.

V. CONCLUSION

In this study, we use a previously established correlation between the IR absorption frequency of the OH-stretching vibration and the corresponding length of the inter-molecular H-bond[54,55] in order to extract the average inter-molecular distance in liquid water in a wide temperature range. For that, the highly structured absorption band of the OH-stretching vibration was unraveled, and several contributions were assigned: the central and most pronounced peak was found to reflect the isolated OH-bond vibration ($\sim$3400 cm^{-1}), and two additional shoulders resemble cooperative vibrations of this highly coupled system of oscillators ($\sim$3250 and $\sim$3550 cm^{-1}). Although alternative views exist that assign each absorption peak to a specific state of a particular number of donors and acceptors of inter-molecular H-bonds,[45–49] several studies interpret considerable contributions to correspond to collective vibrations and combination bands.[24–26,43,50] Our experimental data in a system of dilute OH-bonds (i.e., 2% HDO in D_2O) confirms the latter view by showing a much narrower peak with significantly reduced contributions of these collective vibrations.

The obtained inter-molecular H-bond length of about $\sim$283 pm corresponds well with values reported by past studies using x-ray and neutron scattering,[9,14,15] although the scattering of these and other literature results exceeds the thermal expansion we observe in the investigated temperature interval (260–350 K). A commonly used approach to calculate the average nearest neighbor pair distance of oxygen atoms from the mass density yields about 10 pm lower values and, more importantly, a significantly different temperature dependence, e.g., a clear minimum corresponding to the

density maximum at 277 K in H_2O (284 K in D_2O). In contrast, the inter-molecular H-bond length obtained from the IR data is monotonously increasing in the whole investigated temperature range.

Despite this discrepancy, the extracted inter-molecular H-bond length can be related to the macroscopic mass density through a simple equivalent sphere model with a variable coordination number for adjacent molecules. The resulting values of $\sim$3.5 – 3.6 nearest neighbors in direct contact are well within the expected range.[9,27] This match verifies that the determination of inter-molecular bond lengths from IR absorption frequencies (via a calibrated relation[55]) yields accurate results in the case of inter-molecular H-bonds. However, the need for an additional degree of freedom (i.e., the variable coordination number) in the description demonstrates that the thermal expansion of water consists of two contributions: (i) the structural arrangement of molecules with respect to their neighbors, and (ii) the thermal expansion of the inter-molecular H-bond.

With experimental access to the latter and determination of the overall thermal expansion through mass density, one can extract the purely structural contribution to thermal expansion. As a result, the most compact structure, i.e., considering only molecular arrangements but not the thermal expansion of inter-molecular bonds, is found at considerably higher temperatures than the density maximum, namely, at $\sim$331 K from the experimental data and $\sim$316 K in the simulations. This assignment is corroborated by the coincidence with the temperature of several anomalies related to the susceptibility of the material to pressure; past studies have suggested a single characteristic temperature $T^* \approx 315$ K for all these anomalies.[67,77,78,81] Here, we would like to note that for the determination of T^* through these anomalies, exhaustive measurements in the temperature and pressure parameter spaces have to be carried out. In contrast, with the presented method, it is possible to identify T^* without varying the pressure.

For water, the inter- and intra-molecular bond lengths (and also bond angles for that matter) and their thermal evolution are extremely well-studied via different spectroscopic and other methods,[18–22,65] as well as a multitude of simulations.[20,23–27] However, most other liquids lack such a profound set of data. Thus, we propose a combination of spectroscopic (e.g., FTIR) examination of inter-molecular bond lengths and density/specific volume measurements to disentangle different contributions to thermal expansivity and gain more insight into the correlation of structure and dynamics in disordered systems such as liquids and glasses. Consequently, this method can pave the way to study inter-molecular distances and untangle structural effects—and due to the chemical specificity of IR spectroscopy, even site-specific—in amorphous systems, which are not easily addressed by conventional scattering methods (due to their need for long-range order to address specific bonds).

16 August 2024 13:35:19

AUTHOR DECLARATIONS

Conflict of Interest

The authors have no conflicts to disclose.

Author Contributions

J.P.G. and M.T. contributed equally to this paper.

Jan Philipp Gabriel: Conceptualization (equal); Formal analysis (equal); Funding acquisition (equal); Investigation (equal); Methodology (equal); Project administration (equal); Supervision (equal); Validation (equal); Visualization (equal); Writing – review & editing (equal). **Robin Horstmann**: Data curation (equal); Formal analysis (supporting); Investigation (supporting); Methodology (supporting); Resources (supporting); Software (equal); Validation (supporting); Visualization (supporting); Writing – review & editing (supporting). **Martin Tress**: Conceptualization (equal); Data curation (equal); Formal analysis (equal); Funding acquisition (equal); Investigation (equal); Methodology (equal); Project administration (equal); Resources (equal); Software (equal); Supervision (equal); Validation (equal); Visualization (equal); Writing – original draft (lead); Writing – review & editing (equal).

DATA AVAILABILITY

The data sets generated and analyzed during this study are available from Jan P. Gabriel upon reasonable request.

REFERENCES

[1]X. Xia and P. G. Wolynes, "Fragilities of liquids predicted from the random first order transition theory of glasses," Proc. Natl. Acad. Sci. U. S. A. **97**, 2990–2994 (2000).

[2]J. D. Stevenson and P. G. Wolynes, "Thermodynamic–kinetic correlations in supercooled liquids: A critical survey of experimental data and predictions of the random first-order transition theory of glasses," J. Phys. Chem. B **109**, 15093–15097 (2005).

[3]V. Lubchenko and P. G. Wolynes, "Theory of structural glasses and supercooled liquids," Annu. Rev. Phys. Chem. **58**, 235–266 (2007).

[4]G. Floudas, M. Paluch, A. Grzybowski, and K. Ngai, *Molecular Dynamics of Glass-Forming Systems: Effects of Pressure* (Springer Science & Business Media, 2010), Vol. 1.

[5]S. Pawlus, M. Paluch, and A. Grzybowski, "Communication: Thermodynamic scaling of the Debye process in primary alcohols," J. Chem. Phys. **134**, 041103 (2011).

[6]M. Paluch, E. Masiewicz, A. Grzybowski, S. Pawlus, J. Pionteck, and Z. Wojnarowska, "General rules prospected for the liquid fragility in various material groups and different thermodynamic conditions," J. Chem. Phys. **141**, 134507 (2014).

[7]S. Hensel-Bielowka, S. Pawlus, C. M. Roland, J. Zioło, and M. Paluch, "Effect of large hydrostatic pressure on the dielectric loss spectrum of type-*A* glass formers," Phys. Rev. E **69**, 050501 (2004).

[8]P. Lunkenheimer, A. Loidl, B. Riechers, A. Zaccone, and K. Samwer, "Thermal expansion and the glass transition," Nat. Phys. **19**, 694–699 (2023).

[9]Y. E. Gorbaty and Y. N. Demianets, "An x-ray study of the effect of pressure on the structure of liquid water," Mol. Phys. **55**, 571–588 (1985).

[10]A. H. Narten and H. A. Levy, "Liquid water: Molecular correlation functions from x-ray diffraction," J. Chem. Phys. **55**, 2263–2269 (1971).

[11]T. Head-Gordon and M. E. Johnson, "Tetrahedral structure or chains for liquid water," Proc. Natl. Acad. Sci. U. S. A. **103**, 7973–7977 (2006).

[12]L. Fu, A. Bienenstock, and S. Brennan, "X-ray study of the structure of liquid water," J. Chem. Phys. **131**, 234702 (2009).

[13]Y. I. Naberukhin, "The pair distribution function of liquid water: Truncation problem in light of recent x-ray diffraction data," J. Mol. Liq. **239**, 45–48 (2017).

[14]A. K. Soper, "Joint structure refinement of x-ray and neutron diffraction data on disordered materials: Application to liquid water," J. Phys.: Condens. Matter **19**, 335206 (2007).

[15]U. Bergmann, A. Di Cicco, P. Wernet, E. Principi, P. Glatzel, and A. Nilsson, "Nearest-neighbor oxygen distances in liquid water and ice observed by x-ray Raman based extended x-ray absorption fine structure," J. Chem. Phys. **127**, 174504 (2007).

[16]K. Amann-Winkel, M.-C. Bellissent-Funel, L. E. Bove, T. Loerting, A. Nilsson, A. Paciaroni, D. Schlesinger, and L. Skinner, "X-ray and neutron scattering of water," Chem. Rev. **116**, 7570–7589 (2016).

[17]S. W. Krauss, R. Schweins, A. Magerl, and M. Zobel, "Free-film small-angle neutron scattering: A novel container-free *in situ* sample environment with minimized H/D exchange," J. Appl. Crystallogr. **52**, 284–288 (2019).

[18]T. A. Ford and M. Falk, "Hydrogen bonding in water and ice," Can. J. Chem. **46**, 3579–3586 (1968).

[19]Y. Maréchal, "Infrared spectra of water. I. Effect of temperature and of H/D isotopic dilution," J. Chem. Phys. **95**, 5565–5573 (1991).

[20]S. A. Corcelli and J. L. Skinner, "Infrared and Raman line shapes of dilute HOD in liquid H_2O and D_2O from 10 to 90 °C," J. Phys. Chem. A **109**, 6154–6165 (2005).

[21]L. De Marco, W. Carpenter, H. Liu, R. Biswas, J. M. Bowman, and A. Tokmakoff, "Differences in the vibrational dynamics of H_2O and D_2O: Observation of symmetric and antisymmetric stretching vibrations in heavy water," J. Phys. Chem. Lett. **7**, 1769 (2016).

[22]Y. Zhou, L. Li, Y. Huang, J. Ou, W. Li, and C. Q. Sun, "Perturbative vibration of the coupled hydrogen-bond (O:H–O) in water," Adv. Colloid Interface Sci. **310**, 102809 (2022).

[23]J. Marti, J. Padró, and E. Guàrdia, "Molecular dynamics calculation of the infrared spectra in liquid H_2O–D_2O mixtures," J. Mol. Liq. **62**, 17–31 (1994).

[24]J.-H. Choi and M. Cho, "Computational IR spectroscopy of water: OH stretch frequencies, transition dipoles, and intermolecular vibrational coupling constants," J. Chem. Phys. **138**, 174108 (2013).

[25]Y. Nagata, S. Yoshimune, C.-S. Hsieh, J. Hunger, and M. Bonn, "Ultrafast vibrational dynamics of water disentangled by reverse nonequilibrium *ab initio* molecular dynamics simulations," Phys. Rev. X **5**, 021002 (2015).

[26]S. Carlson, F. N. Brünig, P. Loche, D. J. Bonthuis, and R. R. Netz, "Exploring the absorption spectrum of simulated water from MHz to infrared," J. Phys. Chem. A **124**, 5599–5605 (2020).

[27]J. Liu and X. He, "*Ab initio* molecular dynamics simulation of liquid water with fragment-based quantum mechanical approach under periodic boundary conditions," Chin. J. Chem. Phys. **34**, 761–768 (2021).

[28]C. Gainaru, A. L. Agapov, V. Fuentes-Landete, K. Amann-Winkel, H. Nelson, K. W. Köster, A. I. Kolesnikov, V. N. Novikov, R. Richert, R. Böhmer, T. Loerting, and A. P. Sokolov, "Anomalously large isotope effect in the glass transition of water," Proc. Natl. Acad. Sci. U. S. A. **111**, 17402–17407 (2014).

[29]P. Gallo *et al.*, "Advances in the study of supercooled water," Eur. Phys. J. E **44**, 143 (2021).

[30]G. M. Kontogeorgis, A. Holster, N. Kottaki, E. Tsochantaris, F. Topsøe, J. Poulsen, M. Bache, X. Liang, N. S. Blom, and J. Kronholm, "Water structure, properties and some applications—A review," Chem. Thermodyn. Therm. Anal. **6**, 100053 (2022).

[31]S. Capaccioli, L. Zheng, A. Kyritsis, A. Paciaroni, M. Vogel, and K. L. Ngai, "The dynamics of hydrated proteins are the same as those of highly asymmetric mixtures of two glass-formers," ACS Omega **6**, 340 (2020).

[32]M. Wolf, S. Emmert, R. Gulich, P. Lunkenheimer, and A. Loidl, "Dynamics of protein hydration water," Phys. Rev. E **92**, 032727 (2015).

[33]J. P. Gabriel, M. Tress, W. Kossack, L. Popp, and F. Kremer, "Molecular heterogeneities in the thermal expansivity of polyalcohols," J. Chem. Phys. **154**, 024503 (2021).

[34]R. C. Dougherty and L. N. Howard, "Equilibrium structural model of liquid water: Evidence from heat capacity, spectra, density, and other properties," J. Chem. Phys. **109**, 7379–7393 (1998).

16 August 2024 13:35:19

[35] T.-L. Chang and J.-Y. Chien, "Maximum difference between densities of ordinary and heavy water," J. Am. Chem. Soc. **63**, 1709–1711 (1941).

[36] M. A. González and J. L. Abascal, "A flexible model for water based on TIP4P/2005," J. Chem. Phys. **135**, 224516 (2011).

[37] H. Berendsen, D. van der Spoel, and R. van Drunen, "GROMACS: A message-passing parallel molecular dynamics implementation," Comput. Phys. Commun. **91**, 43–56 (1995).

[38] M. J. Abraham, T. Murtola, R. Schulz, S. Páll, J. C. Smith, B. Hess, and E. Lindahl, "GROMACS: High performance molecular simulations through multi-level parallelism from laptops to supercomputers," SoftwareX **1–2**, 19–25 (2015).

[39] G. Bussi, D. Donadio, and M. Parrinello, "Canonical sampling through velocity rescaling," J. Chem. Phys. **126**, 014101 (2007).

[40] M. Parrinello and A. Rahman, "Polymorphic transitions in single crystals: A new molecular dynamics method," J. Appl. Phys. **52**, 7182–7190 (1981).

[41] T. Darden, D. York, and L. Pedersen, "Particle mesh Ewald: An $N \cdot \log(N)$ method for Ewald sums in large systems," J. Chem. Phys. **98**, 10089–10092 (1993).

[42] D. A. McQuarrie, "The time-correlation function formalism I," in *Statistical Mechanics* (University Science Books, Sausalito, CA, 2000), pp. 467–542.

[43] F. Perakis, L. De Marco, A. Shalit, F. Tang, Z. R. Kann, T. D. Kühne, R. Torre, M. Bonn, and Y. Nagata, "Vibrational spectroscopy and dynamics of water," Chem. Rev. **116**(13), 7590–7607 (2016).

[44] J. Riemenschneider, A. Wulf, and R. Ludwig, "The effects of temperature and H/D isotopic dilution on the transmission and attenuated total reflection FTIR spectra of water," Z. Phys. Chem. **223**, 1011–1022 (2009).

[45] J.-J. Max and C. Chapados, "Isotope effects in liquid water by infrared spectroscopy," J. Chem. Phys. **116**, 4626–4642 (2002).

[46] Q. Sun, "The Raman OH stretching bands of liquid water," Vib. Spectrosc. **51**, 213–217 (2009).

[47] Y. Kataoka, N. Kitadai, O. Hisatomi, and S. Nakashima, "Nature of hydrogen bonding of water molecules in aqueous solutions of glycerol by attenuated total reflection (ATR) infrared spectroscopy," Appl. Spectrosc. **65**, 436–441 (2011).

[48] J.-J. Max and C. Chapados, "Determination of spectroscopic band shapes by second derivatives, Part II: Infrared spectra of liquid light and heavy water," Appl. Spectrosc. **69**, 1281–1292 (2015).

[49] J.-J. Max, P. Larouche, and C. Chapados, "Orthogonalyzed H_2O and D_2O species obtained from infrared spectra of liquid water at several temperatures," J. Mol. Struct. **1149**, 457–472 (2017).

[50] G. R. Medders and F. Paesani, "Infrared and Raman spectroscopy of liquid water through 'first-principles' many-body molecular dynamics," J. Chem. Theory Comput. **11**, 1145–1154 (2015).

[51] D. Sharma, B. Das, and A. Chandra, "Terahertz spectrum of water at varying temperatures from 260 to 340 K: Contributions from permanent and induced dipole correlations at different length scales," J. Phys. Chem. B **127**, 6714–6725 (2023).

[52] K. Zhong, C.-C. Yu, M. Dodia, M. Bonn, Y. Nagata, and T. Ohto, "Vibrational mode frequency correction of liquid water in density functional theory molecular dynamics simulations with van der Waals correction," Phys. Chem. Chem. Phys. **22**, 12785–12793 (2020).

[53] L. De Marco, K. Ramasesha, and A. Tokmakoff, "Experimental evidence of Fermi resonances in isotopically dilute water from ultrafast broadband IR spectroscopy," J. Phys. Chem. B **117**, 15319–15327 (2013).

[54] E. Libowitzky, "Correlation of O–H stretching frequencies and O–H···O hydrogen bond lengths in minerals," Monatsh. Chem. **130**, 1047–1059 (1999).

[55] T. Steiner, "The hydrogen bond in the solid state," Angew. Chem., Int. Ed. **41**, 48–76 (2002).

[56] M. G. Sceats, M. Stavola, and S. A. Rice, "A zeroth order random network model of liquid water," J. Chem. Phys. **70**, 3927–3938 (1979).

[57] M. G. Sceats and S. A. Rice, "The water–water pair potential near the hydrogen bonded equilibrium configuration," J. Chem. Phys. **72**, 3236–3247 (1980).

[58] C. Tulk, D. Klug, R. Branderhorst, P. Sharpe, and J. Ripmeester, "Hydrogen bonding in glassy liquid water from Raman spectroscopic studies," J. Chem. Phys. **109**, 8478–8484 (1998).

[59] D. D. Klug, O. Mishima, and E. Whalley, "High-density amorphous ice. IV. Raman spectrum of the uncoupled O–H and O–D oscillators," J. Chem. Phys. **86**, 5323–5328 (1987).

[60] G. Hura, D. Russo, R. M. Glaeser, T. Head-Gordon, M. Krack, and M. Parrinello, "Water structure as a function of temperature from x-ray scattering experiments and ab initio molecular dynamics," Phys. Chem. Chem. Phys. **5**, 1981–1991 (2003).

[61] R. T. Hart, C. J. Benmore, J. Neuefeind, S. Kohara, B. Tomberli, and P. A. Egelstaff, "Temperature dependence of isotopic quantum effects in water," Phys. Rev. Lett. **94**, 047801 (2005).

[62] A. K. Soper, "An asymmetric model for water structure," J. Phys.: Condens. Matter **17**, S3273 (2005).

[63] A. Soper, "The radial distribution functions of water and ice from 220 to 673 K and at pressures up to 400 MPa," Chem. Phys. **258**, 121–137 (2000).

[64] Y. Huang, X. Zhang, Z. Ma, W. Li, Y. Zhou, J. Zhou, W. Zheng, and C. Q. Sun, "Size, separation, structural order and mass density of molecules packing in water and ice," Sci. Rep. **3**, 3005 (2013).

[65] C. Q. Sun, Y. Huang, X. Zhang, Z. Ma, and B. Wang, "The physics behind water irregularity," Phys. Rep. **998**, 1–68 (2023); a part of Special Issue: The Physics behind Water Irregularity.

[66] S. Herrig, M. Thol, A. H. Harvey, and E. W. Lemmon, "A reference equation of state for heavy water," J. Phys. Chem. Ref. Data **47**, 043102 (2018).

[67] F. Mallamace, G. Mensitieri, D. Mallamace, M. Salzano de Luna, and S.-H. Chen, "Some aspects of the liquid water thermodynamic behavior: From the stable to the deep supercooled regime," Int. J. Mol. Sci. **21**, 7269 (2020).

[68] W. Liu, S. Li, A. Baule, and H. A. Makse, "Adhesive loose packings of small dry particles," Soft Matter **11**, 6492–6498 (2015).

[69] R. M. German, "Coordination number changes during powder densification," Powder Technol. **253**, 368–376 (2014).

[70] T. Steiner and W. Saenger, "Lengthening of the covalent O–H bond in O–H···O hydrogen bonds re-examined from low-temperature neutron diffraction data of organic compounds," Acta Crystallogr., Sect. B: Struct. Sci. **50**, 348–357 (1994).

[71] M. Matsumoto, "Why does water expand when it cools?," Phys. Rev. Lett. **103**, 017801 (2009).

[72] D. Paschek, "How the liquid–liquid transition affects hydrophobic hydration in deeply supercooled water," Phys. Rev. Lett. **94**, 217802 (2005).

[73] D. Liu, Y. Zhang, C.-C. Chen, C.-Y. Mou, P. H. Poole, and S.-H. Chen, "Observation of the density minimum in deeply supercooled confined water," Proc. Natl. Acad. Sci. U. S. A. **104**, 9570–9574 (2007).

[74] H. E. Stanley and J. Teixeira, "Interpretation of the unusual behavior of H_2O and D_2O at low temperatures: Tests of a percolation model," J. Chem. Phys. **73**, 3404–3422 (1980).

[75] A. K. Soper and M. A. Ricci, "Structures of high-density and low-density water," Phys. Rev. Lett. **84**, 2881–2884 (2000).

[76] G. S. Kell, "Density, thermal expansivity, and compressibility of liquid water from 0° to 150° Correlations and tables for atmospheric pressure and saturation reviewed and expressed on 1968 temperature scale," J. Chem. Eng. Data **20**, 97–105 (1975).

[77] F. Mallamace, C. Corsaro, D. Mallamace, C. Vasi, and H. E. Stanley, "The thermodynamical response functions and the origin of the anomalous behavior of liquid water," Faraday Discuss. **167**, 95–108 (2013).

[78] D. Mallamace, C. Corsaro, F. Mallamace, and H. E. Stanley, "Experimental tests for a liquid–liquid critical point in water," Sci. China: Phys. Mech. Astron. **63**, 127001 (2020).

[79] L. S. Shraiber, "Experimental investigation of the thermal dependence of the piezo-optical coefficient of water between 5 and 90 °C," Isr. J. Chem. **13**, 181–184 (1975).

[80] K. E. Bett and J. B. Cappi, "Effect of pressure on the viscosity of water," Nature **207**, 620–621 (1965).

[81] F. Mallamace, C. Corsaro, and H. E. Stanley, "A singular thermodynamically consistent temperature at the origin of the anomalous behavior of liquid water," Sci. Rep. **2**, 993 (2012).

[82] P. H. Poole, F. Sciortino, U. Essmann, and H. E. Stanley, "Phase behaviour of metastable water," Nature **360**, 324–328 (1992).

[83] M. Goldblatt, "The density of liquid T_2O^1," J. Phys. Chem. **68**, 147–151 (1964).

[84] G. Némethy and H. A. Scheraga, "Structure of water and hydrophobic bonding in proteins. IV. The thermodynamic properties of liquid deuterium oxide," J. Chem. Phys. **41**, 680–689 (1964).

16 August 2024 13:35:19